Advances in Differential Equations and Control Processes 2025, 32(4), 3659.
doi: https://doi.org/10.59400/adecp3659

Article

Optimal periodic switching strategy for self-cycling bioprocesses: Fliess series-based parameter design and ethanol fermentation case

Wenliang Li, Chi Zhai*

Faculty of chemical engineering, Kunming University of Science and Technology, Kunming 650500, China

*** Corresponding author:** Chi Zhai, zhaichi@kust.edu.cn

CITATION

Li W, Zhai C. Optimal periodic switching strategy for self-cycling bioprocesses: Fliess series-based parameter design and ethanol fermentation case. Advances in Differential Equations and Control Processes. 2025; 32(4): 3659. https://doi.org/10.59400/adecp3659

ARTICLE INFO

Received: 24 August 2025
Revised: 22 September 2025
Accepted: 25 September 2025
Available online: 8 October 2025

Abstract: This study proposes a framework for optimizing cyclic discharge-reload operations in successive batch bioreactors under integral input constraints (e.g., total substrate consumption, cumulative energy use). Prior research has shown that candidates for optimal fed-batch and periodic on/off operation, formulated in an input-affine system, can be derived from bang-bang form. However, the practical application of these results to successive batch configurations requires a prior knowledge of operational periodicity, which limits flexibility and adaptability to variability. To address this limitation, we reformulate the switching strategy into an algebraic form using the Fliess series expansion. This expansion explicitly embeds periodicity constraints, enabling direct computation of switching parameters from predefined boundary conditions. The overall performance, defined as the over-yield relative to steady-state operations, is quantified via integrated integrals. For practical implementation, we leverage self-cycling fermentation as a foundational framework to determine required periodicity, and design optimal trajectories. Analytical results are derived to clarify the quantitative relationship between boundary conditions and switching parameters for any arbitrary anchor point (i.e., reference state for cycle initialization). The proposed framework is validated using an experimentally calibrated ethanol fermentation model. Simulation results demonstrate that the optimized cyclic strategy achieve a 25.58% relative increase in ethanol yield compared to traditional batch operations. This method enables the seamless integration of on/off operation with optimal periodicity, addressing critical gaps between theoretical periodic switching strategy and industrial bioprocess implementation.

Keywords: Fliess series expansion; periodic optimal control; self-cycling fermentation; bang-bang control; successive batch bioreactors

1. Introduction

In the realm of biomanufacturing, the optimal design of fermentation configurations presents a pivotal challenge, demanding strategies that maximize productivity (e.g., g/L/h) while navigating constraints such as substrate efficiency, equipment costs, and cell viability. A compelling approach lies in successive batch fermentation via cyclic and partial discharge-reload operations, where nonlinear dynamical systems governed by ordinary differential equations (ODEs) under periodic on/off switches are harnessed to enhance performance [1,2].

Early investigations have demonstrated that cyclic strategies, modulating variables like substrate concentration or dilution rate, can outperform steady-state regimes by exploiting transient metabolic dynamics, a phenomenon particularly vital for processes

where peak productivity occurs in non-steady states [3]. For instance, in Monod-type kinetic fermentation, sinusoidal perturbations in substrate feed or dilution rate have been shown to boost mean production rates through the frequency-domain analysis of second-order cost variations [4,5], propelling optimal periodic control (OPC) theory to the interface of mathematics and process engineering [6].

Empirical evidence in applications such as ethanol fermentation has validated that cyclic operations can surpass steady-state counterparts [7]. This has spurred research into unsteady-state strategies for process intensification. Early frameworks relying on Pontryagin's maximum principle (PMP) or relaxed steady-state assumptions derived sufficient conditions for cyclic over-yield near equilibrium [8, 9]. However, these approaches exhibit fundamental limitations: PMP offers qualitative insights but lacks quantitative performance metrics, while steady-state simplifications overlook the critical dynamics of transient phases that often dictate yield maximization.

Refinements using second-order necessary conditions for OPC problems, incorporating state constraints and isoperimetric requirements, introduced the π-test methodology, which applies Laplace transform to linearized systems for periodic perturbation analysis [10]. Despite extending classical variational methods into the frequency domain, practical implementation remains challenging. For instance, in *Saccharomyces cerevisiae* fermentation, reducing the dilution rate to improve substrate conversion paradoxically decreases ethanol yields below batch-mode levels and increases instrumentation costs. This highlights the need for generalized design criteria that can balance multiple objectives.

The generalized Π-criterion [11] represents a significant advancement by enabling the analysis of periodic perturbations around arbitrary stable equilibria in nonlinear systems. It was later extended to multi-source substrate systems via conservation principle-based formulations [12]. However, its reliance on system linearization restricts its validity to small-amplitude inputs, limiting its applicability to processes that require large-scale perturbations for optimal performance.

Subsequent developments, incorporating center manifold approximations [13] and nonlinear parametrization techniques (e.g., Volterra series [14], Laplace-Borel transforms [15]), have improved accuracy under large-amplitude forcing. Methodologies like Carleman linearization [16] and vibration control schemes [17,18] have also expanded the toolkit for stabilizing reactors near unstable equilibria. Multi-frequency averaging extensions and nonlinear frequency response methods [19] have further facilitated stability analysis and time-averaged performance estimation in complex, periodically forced systems.

Constrained-input optimal formulations for fermentation processes have revealed an inherently bang-bang control structure, which is consistent with empirical observations of extended closed-loop operation phases [20]. State-impulsive control strategies for chemostat / turbidostat systems have established rigorous existence conditions and stability criteria for positive periodic solutions (e.g., period-1, period-2 cycles) using Poincaré mapping techniques [21–27]. However, there is still a critical gap in the development of generalized design strategies for fermentation systems subject to integral input constraints (e.g., total substrate usage limits) and undetermined

periodicity. This gap hinders both theoretical progress and experimental realization [28], especially in industrial settings where precise management of cyclic boundary conditions (e.g., batch-to-batch state transitions) is essential for reproducibility and cost-efficiency.

This work aims to address two key challenges: (1) Developing computationally efficient on/off switching protocols for nonlinear input-affine systems with integral constraints, eliminating the need for a priori periodicity assumptions; (2) Theoretically and experimentally characterizing periodic-input fermentation models, focusing on algebraic transformation of affine-input problems via Fliess series, and novel parameter-anchor equation relationships that govern switching dynamics.

Building on the analytical foundations of nonlinear system theory [10], we focus on self-cycling fermentation (SCF) systems. In these systems, cyclic operations can autonomously maintain stable periodic states with minimal external intervention [29,30]. We perform numerical validation using an experimentally calibrated ethanol fermentation model to demonstrate the practical utility of our framework. The remainder of this paper is structured as follows: Section 2 formalizes the control problem with integral constraints. Section 3 details the theoretical developments, including Fliess series-based algebraic reformulation and stability analysis. Section 4 presents simulation results, insights into industrial applicability, and concluding remarks.

2. Process model and problem formulation

2.1. Mathematical model for continuous fermentation processes

This study centers on the optimal cyclic strategy design of successive batch fermentation systems described by ODEs. The motivation is to balance productivity, substrate efficiency, and operational stability in bio-manufacturing. Consider a well-mixed bioreactor without biomass reflux, where the feed stream contains only the limiting substrate S. Key process variables such as liquid volume, pH, temperature, and dissolved oxygen are maintained at optimal set-points through feedback control. This isolates the dynamics of substrate $S(t)$, biomass $X(t)$, and product $P(t)$. The mass balance equations for these species are:

$$\begin{cases} \dfrac{dS}{dt} = D(S_{in} - S) - \sigma[S,P]X \\ \dfrac{dX}{dt} = -DX + \mu[S,P]X \\ \dfrac{dP}{dt} = -DP + \rho[S,P]X \end{cases} \tag{1}$$

where $D = F/V$ is the dilution rate (a manipulated variable with unit of h^{-1}), defined as the ratio of feed flow rate F to reactor volume V; S_{in} is the inlet substrate concentration (in g/L); and σ, μ and ρ denote the specific rates of substrate consumption, biomass growth, and product formation, respectively. Microbial growth is modeled using a modified Monod equation that incorporates product inhibition, which is crucial for ethanol fermentation as accumulated product (e.g., ethanol) suppresses biomass growth:

$$\mu[S,P] = \frac{\mu_m S}{K_s + S} \cdot \frac{K_i}{P + K_i}, \tag{2}$$

where μ_m is the maximum specific growth rate (h^{-1}), K_s is the substrate half-saturation constant (g/L), and K_i is the product inhibition constant (g/L). Substrate consumption and product formation are assumed to be proportional to biomass growth via yield coefficients: $Y_{xs} = \mu/\sigma$, $Y_{xp} = \mu/\rho$.

At steady state ($d/dt = 0$), the system admits two equilibrium solutions: (1) Trivial solution (washout state), (S, X, P) = (S_{in}, 0, 0), where biomass is absent; (2) Non-trivial solution (productive state), (S^*, X^*, P^*), which satisfies:

$$D = \mu^*[S^*, P^*]; S^* = \frac{K_s D}{\mu_m - D}; P^* = K_i \sqrt{\frac{\mu_m - D}{D} - \frac{K_s}{S_{in}}} \tag{3}$$

Stability analysis of the linearized system around (S^*, X^*, P^*) yields the characteristic equation:

$$\lambda(\lambda + D/Y_{xy})(D + \lambda - \mu) = 0. \tag{4}$$

The dominant eigenvalue $\lambda_2 = \mu - D$ dictates stability: (1) When $D > D_c = \mu_m S_{in}/(S_{in} + K_s)$, $\lambda_2 < 0$, and the trivial solution is stable (washout occurs); (2) For $D < D_c$, $\lambda_2 > 0$, and the non-trivial solution becomes locally stable, with biomass and product accumulating.

Steady-state operation under $D < D_c$ presents inherent limitations that hinder industrial feasibility. First, reducing D extends residence time, which increases capital expenditures (e.g., reactor volume requirements) without commensurate gains in product yield. Second, downstream processing complexity escalates, as the high product concentrations associated with low dilution rates impose significant challenges for separation and purification (e.g., increased energy demands for distillation or chromatography). Batch and fed-batch modes, while effective for achieving high product titers, are constrained by substantial downtime between production runs. This downtime, required for harvesting, cleaning, sterilization, and re-inoculation, reduces overall process throughput and elevates labor and operational costs. These combined limitations motivate the development of optimal cyclic discharge-reload strategies, herein referred to as successive batch fermentation. This approach leverages on/off modulation of D to preserve the high-titer advantages of batch fermentation while enabling periodic broth exchange to maintain cell viability, enhances productivity under integral input constraints (e.g., total substrate utilization, energy limits).

2.2. Optimal cyclic design with integral constraint on the input

In this section, we formulate the OPC problem for systems operating around a steady-state fixed point (u^*, x^*), where $u(t)$ represents the control input and $x(t) \in \mathbb{R}^n$ represents the state vector. The objective is to design a τ-periodic control $u(t)$ that minimizes the time-averaged performance while satisfying integral constraints on the input and periodicity of the state trajectory.

$$\begin{aligned} \min_{u(t),x(t),\tau} \quad & J(u,x,\tau) = \frac{1}{\tau}\int_0^\tau \varphi(x(t),u(t))\,dt, \\ \text{s.t.} \quad & \left| \begin{array}{l} \dfrac{dx}{dt} = f(x(t),u(t)), \\ x(0) = x(\tau), \\ u^* = \dfrac{1}{\tau}\int_0^\tau u(t)\,dt. \end{array} \right. \end{aligned} \tag{5}$$

where $J(u,x,\tau)$ is the instantaneous performance metric, $f(u,x)$ describes the process dynamics, and $\tau > 0$ is the fixed period. The control input $u(t)$ is τ-periodic, i.e., $u(t+\tau) = u(t)$ for all $t > 0$.

Physically, this problem aims to minimize the average substrate loss S by regulating the input such that the total substrate consumption over $t \in (0,\tau)$ remains constant. For the steady-state solution $u(t) = u$, the periodicity constraint $x(0) = x(\tau)$ is trivially satisfied, and $J(u^*,x^*,\tau) = \phi(u^*,x^*)$ due to the absence of time-varying dynamics. A key objective of cyclic operation is to construct $u(t)$ such that $J(u,x,\tau) < \phi(u^*,x^*)$, thus achieving an over-yield relative to the steady-state operation through periodic time-varying input strategies.

To analyze the OPC problem for fermentation process described by Eqs. (1)–(2), PMP is employed. This introduces the Hamiltonian function:

$$H(u,x,\lambda) = \phi(u,x) + \lambda^T f(u,x), \tag{6}$$

where $\lambda(t) \in R^n$ is the adjoint vector associated with the state dynamics. Under normal circumstances (no terminal costs), the periodicity constraint $x(0) = x(\tau)$ implies $\lambda(0) = \lambda(\tau)$ for the adjoint variables. For problems with integral constraints on $u(t)$, $\int_0^\tau u(t)dt = K$ (i.e., fixed total input over the period), in the domain $[0,\tau]$, we introduce an auxiliary state $z(t) = \int_0^t u(t)dt$ with dynamics $\dot{z} = u(t)$ and a terminal constraint $z(\tau) = K$. The augmented Hamiltonian then becomes:

$$H(u,x,z,\lambda,\nu) = \varphi(u,x) + \lambda^T f(u,x) + \nu u \tag{7}$$

where ν is the adjoint variable for the auxiliary state z.

The optimal control $u(t)$ is determined by maximizing H point-wise in time. this leads to two possible regimes: (1) Bang control, where the control takes extreme values $u_{\max}$ or $u_{\min}$ when $\frac{\partial H}{\partial u} \neq 0$, In this case, the Hamiltonian is maximized at the boundary of the control set. (2) Singular control, if $\frac{\partial H}{\partial u} = 0$ over an interval (i.e., the control is interior to the allowable set), higher-order conditions (e.g., differentiating $\frac{\partial H}{\partial u}$ with respect to time) are required to characterize the control law. In previous study [31], it was shown that when the specific growth kinetics $\mu(S)$ in fermentation models is convex, the singular arc does not exist, reducing the optimal strategy to a bang-bang form. This result arises because convexity ensures that the second derivative $\frac{\partial^2 H}{\partial u^2} > 0$, making the Hamiltonian strictly convex in u. As a result, the extremum cannot occur in the interior of the control set, eliminating the possibility of singular segments. The absence of singular arcs simplifies the control synthesis, as the optimal input is fully characterized by its boundary values and switching instants, avoiding the need for

solving higher-order differential equations associated with singular control.

For the bang-bang case, the control alternates between u_{max} and u_{min} at switching times determined by the sign of the switching function $\sigma(t) = \frac{\partial H}{\partial u}$. Given the convexity of $\mu(S)$, $\sigma(t)$ is a monotonic function of time, resulting in a finite number of switches over $[0, \tau]$. The periodicity constraint $x(0) = x(\tau)$ poses a boundary-value problem on the state and adjoint trajectories, and is solved analytically in this work.

3. Main results

In this section, we characterize the optimal on/off strategy for general input-affine systems with integral constraints on the input, extending the framework introduced in Section 2.2. We focus on systems decomposed into the form:

$$\begin{cases} \dfrac{dx}{dt} = f(x) + ug(x), \quad x = (x_1, ..., x_n)^T \in X,\ u = (u_1, ..., u_m)^T \in U \\ y(t) = \varphi_x(t) \end{cases} \tag{8}$$

where $f, g : R^n \to R^n$ are analytic vector fields with continuous derivatives in x, and the input $u(t)$ takes values in a compact set $U = [u_{\min}, u_{\max}] \subset R$. The objective is to minimize time-averaged output $y(t) = \phi(x(t))$ under integral constraint:

$$\frac{1}{\tau}\int_{t_0}^{t_0+r} udt = u^* \tag{9}$$

and the periodic boundary condition:

$$x^0 = x(t_0) = x(\tau + t_0), \tag{10}$$

where $\tau > 0$ is the fixed period, and $x^0 = x(t_0)$ anchors the trajectory on a closed oscillatory orbit. Here, x^0 denotes the initial state at $t = t_0$, ensuring the trajectory evolves on a periodic orbit.

To obtain the optimal condition with explicit design of the periodicity, we discretize the periodic orbit. Consider a positive integer $N > 0$ and a partition of the time interval $[t_0, \tau + t_0]$ into N subintervals $[t_{j-1}, t_j)$, where $t_j = t_0 + \sum_{k=1}^{j} \tau_k$ and $\tau_k > 0$ is the duration of the k-th sub-interval. Assume the control input $u(t)$ is piece-wise constant, taking values $u_j \in U$ on $[t_{j-1}, t_j)$, such that:

$$u(t) = \sum_{j=1}^{N} u_i \chi_{\{t_{j-1}, t_j\}}(t), \tag{11}$$

where $\chi_{[t_{j-1}, t_j)}(t)$ is the indicator function (1 for $t \in [t_{j-1}, t_j)$, 0 otherwise). If this discretized control law is optimal, the cost functional:

$$J[x] = \frac{1}{\tau}\int_{t_0}^{t_0+\tau} \varphi(x(t), u(t))dt \tag{12}$$

must be minimized over all admissible N and partitions $\{\tau_j\}$ satisfying constraints (9) and (10).

Substituting (11) into (8), the system reduces to a driftless concatenation of vector

fields over each subinterval:

$$\frac{dx}{dt} = \sum_{j=1}^{N} \chi_{[t_{j-1},t_j]}(t)\Big(f(x) + u_j g(x)\Big) \text{for } j = 1, 2, ..., N \tag{13}$$

For each subinterval $[t_{j-1}, t_j)$, the solution to this Cauchy problem with initial state x^0 is denoted by the flow map:

$$x_{[t_{j-1},t_j)}(t) = \exp(t - t_{j-1})(f(x) + u_j g(x))x^0 \tag{14}$$

where $\exp(\cdot)$ represents the exponential map of the vector field. To satisfy the periodic boundary condition (10), the Fliess functional expansion [32] is employed to approximate the solution as a nested series of Lie brackets, ensuring

$$\exp(\tau_N(f + u_N g)) \circ ... \circ \exp(\tau_1(f + u_1 g))(x^0) = x^0 \tag{15}$$

Notably, the recursively nested structure of (15) preserves the fixed ordering of the left-hand side composition, a critical property for maintaining periodicity.

3.1. Heuristic introduction of Fliess expansion

Given that the scalar function $y(t) = \phi(x(t))$ is analytic, one can expand $y(t)$ at $t = 0$ using the Taylor series. Subsequently, we can transform this Taylor-series expansion into a form of iterated integrals. The expansion is given by:

$$y(t) = \sum_{i=1}^{n} a_i \frac{t^i}{i!} + R_n \approx \sum_{i=1}^{n} a_i \int_0^t d\xi_i \cdots d\xi_0 \tag{16}$$

where R_n is the residual term, and a_i is the i-th order derivative of $y(t)$ evaluated at $t = 0$, i.e., $a_i = y^{(i)}(0)$. When ϕ is considered as a function of x, the coefficients a_i take on the form of Lie derivatives. One then obtain:

$$y(t) = \varphi(\mathbf{x}^0)\left[1 + \sum_{\nu=0}^{\infty} \sum_{i,...,l=1}^{N} L_{f_i} \cdots L_{f_\nu} \int_0^t d\xi_{i_k} \cdots d\xi_{i_l}\right], t \in [0, \tau] \tag{17}$$

Here, L denotes the Lie derivative. The equivalence of the expansion in Equation (16) is established based on the Peano-Baker principle. This principle is particularly useful as the solution to ordinary differential equations (ODEs) can be elegantly represented in terms of iterated integrals.

As an illustration, let's consider a linear differential equation of the form:

$$\frac{dx(t)}{dt} = y(t)x(t) \tag{18}$$

where $y(t)$ is a continuous function over a finite time interval $[0, T]$. One can use the method of successive approximations with the recurrence relations:

$$x^k(t) = x(0) + \int_0^t y(t)x^{k-1}dt \tag{19}$$

The solution of this linear time-variant system can be expressed as:

$$\begin{aligned} x &= x(0)\Big[1 + \textstyle\int_0^t y(\alpha)d\alpha + \int_0^t y(\alpha)\int_0^\alpha y(\beta)d\beta d\alpha + \cdots\Big] \\ &= x(0)\Big[1 + \sum_{i=0}^{\infty} c_i \textstyle\int_0^t d\xi_i \cdots d\xi_0\Big] \end{aligned} \tag{20}$$

where c_i represent the coefficients of the integrated integrals.

If $y(t)$ is a nonlinear function, the solution can still be written in terms of iterated integrals. However, the recurrence relations need to be modified accordingly:

$$x^k(t) = x(0) + \int_0^t y(x^{k-1}, t)dt \tag{21}$$

This approach is the foundation of Picard's method [33]. The convergence properties of these series solutions are presented in **Theorem 1**.

Theorem 1. *Suppose there exists a real positive number M such that the coefficients c_i of the iterated integrals in Eq. (20) satisfy the growth relation $|c_i| < (i+1)!M^{i+1}$, then the series (22) is uniformly and absolutely convergent in some finite time interval $[0, T]$.*

Proof of Theorem 1. From the definition of the iterated integral (19) one has

$$\int_0^t d\xi_i \cdots d\xi_0 < \frac{t^{i+1}}{(i+1)!} \tag{22}$$

Then, when the growth condition is satisfied,

$$\left|\int_0^t c_t d\xi_t \cdots d\xi_0\right| < (Mt)^{t+1} \tag{23}$$

It follows that for T sufficiently small, the series (19) is uniformly convergent in $t \in [0, T]$. □

This heuristic introduction provides an intuitive understanding of how the Fliess expansion builds upon well-known concepts in the solution of differential equations, such as Taylor series, Lie derivatives, and Picard's method of successive approximations.

3.2. Switching design

Let's return to the original problem (5), Specifically, the state $x(t)$ is expressed as:

$$x(t) = x^0 + \sum_{i=1}^{N}(f+u_i g)\Big|_{x^0} V_i(t) + \sum_{i,j=1}^{N} L_{f+u_i g}\Big(f+u_i g\Big|_{x^0} V_{ij}(t) + \sum_{i,j,l=1}^{N} L_{f+u_i g}L_{f+u_j g}\Big(f+u_i g\Big|_{x^0} V_{ijl}(t) + R(t) \tag{24}$$

where

$$
\begin{aligned}
V_i(t) &= \int_0^t d\alpha \\
V_{ij}(t) &= \int_0^t \int_0^\beta d\beta d\alpha \\
V_{ijl}(t) &= \int_0^t \int_0^\beta \int_0^\chi dz d\beta d\alpha
\end{aligned} \tag{25}
$$

Once $x(t)$ is determined, one can construct piece-wise constant controls u_i and find the solutions $x(t = \tau)$ to satisfy the boundary constraint (10). The integral constraint can be reduced to follows,

$$
\sum_{i=1}^{N} \tau_i u_i = \tau u^*, \;\; \tau_i = t_i - t_{i-1} > 0 \tag{26}
$$

Since the time response is only related to $V(t)$, direct computation of the integrals in (24) leads to:

$$
\begin{aligned}
V_i(t) &= \begin{cases} 0 & t \le t_{i-1} \\ t - t_{i-1} & t \in (t_{i-1}, t_i) \\ \tau_i & t \ge t_i \end{cases} \\
V_{ii}(t) &= \begin{cases} 0 & t \le t_{i-1} \\ (t - t_{i-1})^2/2 & t \in (t_{i-1}, t_i) \\ \tau_i^2/2 & t \ge t_i \end{cases} \\
V_{ij}(t) &= \begin{cases} 0 & t \le t_{i-1} \\ (t - t_{i-1})\tau_j & t \in (t_{i-1}, t_i), \text{ for} \, i > j \\ \tau_i \tau_j & t \ge t_i \end{cases}
\end{aligned} \tag{27}
$$

Higher-order iterated integrals can be obtained through further integration. For example:

$$
V_{ijl}(t) = \int_0^t V_{jl} d\alpha, V_{ijl}(\tau) = \int_{t_{i-1}}^{t_i} V_{jl} d\alpha \tag{28}
$$

After that, the approximation procedure in (24) needs to be appropriately assessed, which is valid when $f + u_j g$ are $C^k(x)$, where k is the order of expansion. The remainder term $R(\tau)$ satisfies the estimate $R(\tau) = O(\tau^4)$, and the proof is provided [34]. Thus, for $x(t = \tau) = x^0$, one has the following relation:

$$
\begin{aligned}
\sum_{i=1}^{N} (f + u_i g)\Big|_{x^0} \tau_i + \sum_{i=1}^{N} \frac{\tau_i^2}{2} L_{f+u_i g}(f + u_i g)\Big|_{x^0} + \sum_{1 \le j \le N} \tau_i \tau_j \, (f + u_i g) \, \Big|_{x^0} + \\
\sum_{i,j,l=1}^{N} L_{f+u_i g} L_{f+u_i g}(f + u_i g)\Big|_{x^0} \int_{t-1}^{t} V_{jl} d\alpha = O(\tau^4)
\end{aligned} \tag{29}
$$

Moreover, for time-average performance $ave(x)$, such as the overall production, considering equations (9) and (10), equation (24) becomes:

$$\begin{aligned}\text{ave}(x) = \frac{1}{\tau}\int_0^\tau x(t)dt = x^0 + \frac{1}{2\tau}\sum_{i=1}^{N}\tau_i(\tau_i + 2(\tau-\tau_i))(f+u_ig)\big|_{x^0} \\ + \frac{1}{6\tau}\sum_{i=1}^{N}\tau_i^2(\tau_i + 3(\tau-\tau_i))L_{f+u_ig}(f+u_ig)\big|_{x^0} \\ + \sum_{1\le j<i\le N}\tau_i\tau_j(\tau_i + (\tau-\tau_i))L_{f+u_ig}(f+u_ig)\big|_{x^0} + O(\tau^3)\end{aligned} \tag{30}$$

By parameterize the switching times as:

$$\begin{aligned}&\tau_j = \alpha_j\tau, \quad \alpha_j > 0, \quad j = 2,...,N, \\ &\tau_1 = \left(1 - \sum_{j=2}^{N}\alpha_i\right)\tau > 0\end{aligned} \tag{31}$$

the integral constraint on the input yields,

$$u^* = u_1 + \sum_{j=2}^{N}\alpha_j(u_i - u_1) \tag{32}$$

and (32) turns to

$$\begin{aligned}&(f+u_1g)|_{x^0} + \sum_{j=2}^{N}\alpha_j(u_jg - u_1g)|_{x^0} + \frac{\tau}{2} \\ &\left\{\begin{array}{l} L_{f+u_1g}(f+u_1g)|_{x^0} + 2\sum_{j=2}^{N}\alpha_j L_{f+u_jg}(u_jg-u_1g)|_{x^0} \\ + \sum_{j=2}^{N}\alpha_j^2\left(L_{f+u_1g}(u_1g - f - 2u_jg)|_{x^0} + L_{f+u_1g}(f+u_jg)|_{x^0}\right) \\ + 2\sum_{2\le j<i\le N}\alpha_i\alpha_j\left(L_{f+u_1g}(u_1g - f - u_ig - u_jg)|_{x^0} + L_{f+u_1g}(f+u_ig)|_{x^0}\right)\end{array}\right\} \\ &= o(\tau^2)\end{aligned} \tag{33}$$

While (30) becomes,

$$\begin{aligned}\text{ave}(x) = x^0 + \frac{\tau}{2}\left\{(f+u_ig)\big|_{\chi^0} + \sum_{j=2}^{N}\alpha_j\left(\alpha_j + 2\sum_{i=j+1}^{N}\alpha_i\right)(u_j-u_i)g\big|_{\chi^0}\right\} \\ + \frac{\tau^2}{6}\left\{\begin{array}{l} L_{f+u_ig}(f+u_1g)\big|_{\chi^0} + 3\sum_{j=2}^{N}\alpha_j\left(\alpha_j + 2\sum_{i=j+1}^{N}\alpha_i\right)L_{f+u_ig}(u_j-u_i)g\big|_{\chi^0} \\ + \sum_{j=2}^{N}\alpha_j^2\left(\alpha_j + 3\sum_{i=j+1}^{N}\alpha_i\right)\left(L_{f+u_1g}(2u_1-3u_j-f)g\big|_{\chi^0} + L_{f+u_jg}(f+u_jg)\big|_{\chi^0}\right) \\ + 6\sum_{2\le i<j\le N}\alpha_i\alpha_j\alpha_l\left(L_{f+u_1g}(2u_1-2u_i-u_j-f)g\big|_{\chi^0} + L_{f+u_1g}(f+u_jg)\big|_{\chi^0}\right) \\ + 3\sum_{2\le i<j\le N}\alpha_i\alpha_j^2\left(L_{f+u_1g}(2u_1-2u_i-u_j-f)g\big|_{\chi^0} + L_{f+u_1g}(f+u_jg)\big|_{\chi^0}\right)\end{array}\right\} + O(\tau^3)\end{aligned} \tag{34}$$

In particular, when we assume $N = 2$ and for the on/off switching setting where $u_1, u_2 \ge 0$, we have,

$$ave(u) = \alpha_1 u_{\max} + \alpha_2 u_{\min} \tag{35}$$

and

$$\begin{aligned} O(\tau^2) = &(f + (1-\alpha_2)u_1 g + \alpha_2 u_2 g)|_{\chi^0} \\ &+ \frac{\tau}{2}\left\{L_{f+u_1 g}(f+u_1 g)|_{\chi^0} + 2\alpha_2 L_{f+u_1 g}(u_2 - u_1)g|_{\chi^0}\right. \\ &\left.+\alpha_2^2\left(L_{f+u_1 g}(u_1 g - f - 2u_2 g)|_{\chi^0} + L_{f+u_2 g}(f+u_2 g)|_{\chi^0}\right)\right\} \end{aligned} \tag{36}$$

$$\begin{aligned} \text{ave}(x) = &x^0 + \frac{\tau}{2}\left\{(f+u_1 g)|_{\chi^0} + \alpha_2^2(u_2 - u_1)g|_{\chi^0}\right\} \\ &+ \frac{\tau^2}{6}\left\{L_{f+u_1 g}(f+u_1 g)|_{\chi^0} + 3\alpha_2^2 L_{f+u_1 g}(u_2 - u_1)g|_{\chi^0}\right. \\ &\left.+\alpha_2^3\left(L_{f+u_1 g}(2u_1 - 3u_2 - f)g|_{\chi^0} + L_{f+u_2 g}(f+u_2 g)|_{\chi^0}\right)\right\} + O(\tau^3) \end{aligned} \tag{37}$$

To apply above results, the periodicity τ need to be known *a priori*. Moreover, if the analytical representation in (24) is for the scenario of successive batch-to-batch fermentation, the initial states $x^0(t = t_0)$ should lie on the orbit. This further requires the system to converge to the periodic trajectory under external periodic forcing. Other issues such as the number of switching within one period and the optimality condition make the application of these results challenging. Therefore, we will focus on the process and take practical issues into account.

4. Optimal on/off switching strategy for successive batch-to-batch bioprocesses

To anchor the theoretical framework of optimal on/off switching within a practical bioprocessing context, we adopt self-cycling fermentation (SCF) as a prototypical model for successive batch-to-batch production. As illustrated in **Figure 1**, SCF is a cyclic, semi-continuous bioprocessing technique that operates over multiple identical cycles, each involving a controlled discharge-and-reload phase [35]. Our framework aligns with SCF dynamics, where the strategy triggers at the onset of the stationary phase: half of the culture volume is automatically removed for downstream processing and replaced with fresh medium to initiate the next cycle. This operation is executed under a fixed maximum dilution rate $D = D_{\max}$, distinguishing it from conventional SCF by emphasizing periodic on/off switching as a control mechanism.

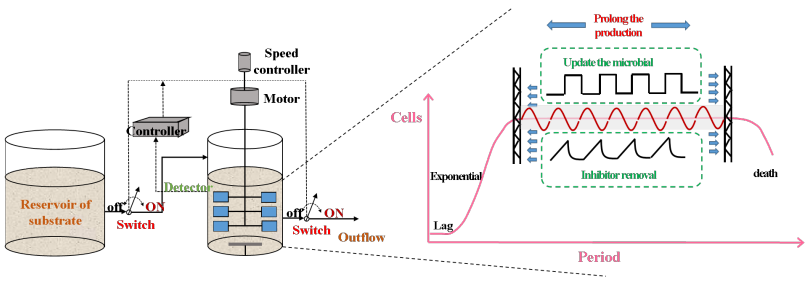

Figure 1. A schematic presentation of SCF apparatus.

Note: The switch system triggers the discharge-and-reload of the substrate to update the culturing media.

SCF represents an intermediate operational mode between fully batch and continuous bioprocesses, integrating advantages of both while mitigating their limitations. Unlike traditional batch fermentation, SCF obviates time-intensive inoculation and seeding procedures, as well as the downtime associated with post-harvest cleaning, sterilization, and reconfiguration. By initiating each cycle in batch mode and implementing periodic, automated discharge-reload operations, and with minimal interference to the culturing system, SCF maintains the dynamic behavior of batch processes (e.g., distinct growth phases and product formation kinetics) while enabling near-continuous operation. This design preserves the high product titers characteristic of batch systems and circumvents the instability challenges inherent in chemostats [36], where small perturbations can disrupt microbial populations or metabolic pathways.

In continuous bioprocessing, efforts to align the dilution rate with slow fermentation kinetics (e.g., in ethanol production) often necessitate reducing throughput, which can lower product titers below batch-mode levels. Industrial attempts to mitigate substrate loss via cascaded multi-tank configurations introduce additional complexities, such as unpredictable fluctuations in bioreactor outlet stream composition and susceptibility to catastrophic failures: a single-tank malfunction in a cascaded system can propagate errors, forcing complete process shutdown. These stability and reliability issues underscore the limitations of purely continuous approaches, even when optimized for efficiency.

By contrast, SCF's periodic on/off switching strategy, triggered at physiologically optimal points (e.g., the onset of the stationary growth phase), offers a robust alternative. This strategy involves removing a fixed volume of culture (e.g., 50%) for downstream processing and replenishing it with fresh medium, resetting substrate availability while retaining established biomass. Such discrete, controlled interventions avoid the steady-state oscillations of continuous systems and leverage the reproducibility of batch dynamics, ensuring consistent performance across cycles. The resulting operational framework characterized by closed-loop periodicity and minimal inter-cycle disruption, provides a viable foundation for optimizing productivity, yield, and resilience in bio-manufacturing.

Given these distinctions, this work focuses on designing periodic on/off switching strategies for SCF, leveraging the theoretical framework of optimal control introduced in Section 3. The goal is to formalize the optimization of switching timing and operational parameters, ensuring convergence to periodic trajectories while maximizing process efficiency under practical constraints (e.g., cycle time, volume exchange ratio, and event-triggering thresholds).

4.1. Modeling and the design issues

To validate the model parameters, SCF experiments are employed. As previously noted, the dynamics of SCF closely resemble those of batch-mode fermentation; thus, data from batch experiments [37] are utilized for the regression process. As exhibited in **Figure 2**, conservation relations for different substances are fitted against time, and kinetic parameters, including the maximum specific growth rate $\mu_m = 0.605\ \mathrm{h}^{-1}$,

substrate half-saturation constant $K_s = 1.73$ g/L, and inhibition constant $K_i = 3.89$ g/L, are estimated via least-square regression on field data. This involves solving the ordinary differential equations (ODEs) (1)–(2) with these unknown parameters. The optimal regression results are depicted in **Figure 2a**. The model is subsequently validated using 21-cycle SCF experiments (Wang et al., 2020), with **Figure 2b** demonstrating its strong performance in describing the SCF process.

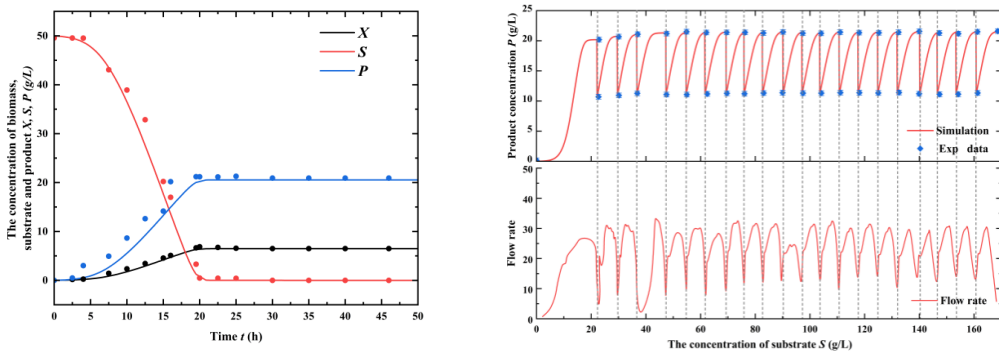

(a) **(b)**

Figure 2. Experimental validation of the ethanol fermentation process: **(a)** Fitting of the kinetics of Eq. (2) using batch fermentation data; **(b)** Verification on the SCF experiment.
Note: Carbon evolution rate (CER) decay is the triggering signal for the experiment and TTM is adopted for the simulation, based on the process model (1), and the $r = 0.5$ with discharge-and-reload interval for 5 minutes.

For constant yield coefficients Y_{xs} and Y_{xp}, the relation $X(t) = P(t)/Y_{xp}$ holds under identical initials $X^0 = P^0$, where the batch fermentation starting point approximates $X^0, P^0 \to 0$, reducing system (1) to a two-dimensional system. Defining $z := Y_{xs}(S_{in} - S) - X$, the ODE $z' = -Dz$ is derived, which converges to zero. If z = 0 holds identically, equations (1) and (2) simplify to a one-dimensional system:

$$\begin{aligned} &\frac{dS}{dt} = \big(D(t) - \nu(S)\big)(S_{in} - S), \\ &\text{where: } \nu(S) := \mu(S, P(S)) = \frac{\mu_m S}{k_s + S} \cdot \frac{K_i}{Y_{xs}(S_{in} - S)/Y_{sp} + K_i}. \end{aligned} \tag{38}$$

Based on this model development, theorems regarding over-yield and stability are established to inform the design of periodic on/off switching strategies.

Lemma 1. *For the nonlinear control-affine system (8) with an integral constraint on the input (9), if (10) converges with τ-periodicity, the optimal solution to (5) is a bang-bang control with exactly two switching times.*

Proof of Lemma 1. See Reference (Bayen et al., 2020). To apply **Lemma 1** to our system, consider $f, g : R \to R$ as C^1 satisfying:

- **H1:** g is positive on I, $f(a) - g(a) = 0$ and $f(b) + g(b) = 0$;
- **H2:** $f - g < 0$ and $f + g > 0$ on $I = (a, b)$;
- **H3:** There exists $ave(x) \in I$ such that $\phi(ave(x)) = ave(u)$, where $\phi := -f/g$, satisfying $\phi(x) - \phi(ave(x)) - \phi'(ave(x))(x - ave(x)) > 0$;
- **H4:** ϕ is increasing on I, and ϕ^{-1} is strictly convex increasing on $\phi(I)$.

Let I denote the largest open set containing ave(S), which is an invariant set for Eq. (31) under controls in $[D_{\min}, D_{\max}]$. Define $u := \alpha D + \beta \in [-1, 1]$, where $\alpha := 2/(D_{\max} - D_{\min})$ and $\beta := -(D_{\max} + D_{\min})/(D_{\max} - D_{\min})$. Setting $f(S) := (-\phi(S) - \beta/\alpha)(S_{in} - S)$, $g := (S_{in} - S)/\alpha$, $\phi(S) := \mu(S)$ and $\psi(S) := \alpha\nu(S) + \beta$, conditions H1–H2 are satisfied. Convexity of $\phi(S)$ and fulfillment of H3–H4 are readily verified. Thus, the switching count is $N = 2$ for the current case. Setting $D_{\min} = 0$ due to the practical consideration that fermentation rates are negligible compared to dilution rates, problem (5) reduces to designing a periodic on/off switching strategy. □

4.2. Numerical simulation and discussion

Previous SCF is set as the event-triggering strategy, where cell density reaching maximum X_c triggers the discharge-and-refill actions, and it is applicable in real-time practice by monitoring X_c through signal of carbon evolution rate (CER) decay, as is exhibited in **Figure 2b**. However, the optimization problem concerning the cycling period is still a challenging task. In the following numerical simulation, the process model (38) is assumed to be accurate and the control is performed under a time-triggering mechanism. Then on/off switching operation with two switching events over a period τ gives:

$$D(t) = \begin{cases} D_{\max} : t \in [0, t_1] \cup (t_2, \tau]; \\ D_{\min} : t \in (t_1, t_2). \end{cases} \tag{39}$$

where the switching time point t_1 and t_2 satisfy:

$$\begin{cases} (\tau - t_2 + t_1) D_{\max} = \text{ave}(D)\tau; \\ \int_0^{\tau} v(S(t))dt = \text{ave}(D). \end{cases} \tag{40}$$

Over-yield condition is derived using Eq. (37). For instance, setting the average dilution rate $ave(D) = 0.0878\ \text{h}^{-1}$ yields the steady-state substrate concentration $S^* = 20.58$ g/L. With $\tau = 11.5$ h, $u_1 = D_{\max} = 0.3\ \text{h}^{-1}$ and $u_2 = D_{\min} = 0\ \text{h}^{-1}$. Eq. (35) gives $\tau - t_2 + t_1 = 1.01$ h, and Eq. (37) becomes:

$$ave(S) = S^* + \frac{\tau}{2}\{f\big|_{S^*} - \alpha_2^2\, g\big|_{S^*}\} + \frac{\tau^2}{6}\{L_{f+g}(f+g)\big|_{S^*} - 3\alpha_2^2 L_{f+g}\, g\big|_{S^*} + \alpha_2^3(L_{f+g}\,(2-f)g\big|_{S^*} + L_f f\big|_{S^*}\} \tag{41}$$

where $\alpha_2 = 0.912$ indicates a highly asymmetric switching profile. The discharge-reload ratio is approximately 50% (v/v), and the average substrate discharge is 18.78 g/l, that is, an 8.7% (w/w) reduction in substrate loss compared to steady-state operation at $D = ave(D)$. Solving Eqs. (39) and (40) yields optimal switching times (t_1, t_2) = (0.52, 11.01) h. This results provides insights into possible on/off switching strategy design.

Maximizing productivity alone might prioritize high $\nu(S)$, which corresponds to high dilution rates. However, excessively high D risks washout in continuous systems and increases substrate loss and ethanol purification costs, both industrially

impractical. The goal here is to mimic SCF behavior under on/off switching: seamless batch-to-batch operation without manual intervention, maximizing substrate depletion to enhance conversion and minimize downstream separation burdens. This requires alignment with industrial feasibility.

Periodicity significantly influences over-yield. As shown in **Figure 3**, an optimal period is necessary to maximize productivity, reaching 0.6 (g/l h) at $\tau = 13$ h. Substrate conversion increases with τ, achieving a 43.4% loss reduction compared to steady-state operation at $\tau = 20$ h. However, the current model (1) does not account for potential cell viability decline during long-term fermentation, introducing a practical constraint. It is hypothesized that the accumulation of secreted ethanol triggers end-product inhibition [31, 38], which is to be avoided for SCF, and Astudillo et. al. [36] suggested $\tau < 20$ h to avoid possible problem of cell viability decline during SCF design. Thus, an optimal period exists for the on/off strategy; we recommend $\tau \in [13, 20]$ h, where high productivity coincides with robust conversion. Shorter periods risk increased substrate loss, while excessively long periods neglect biological limitations, highlighting the need for balanced design across operational and biological constraints.

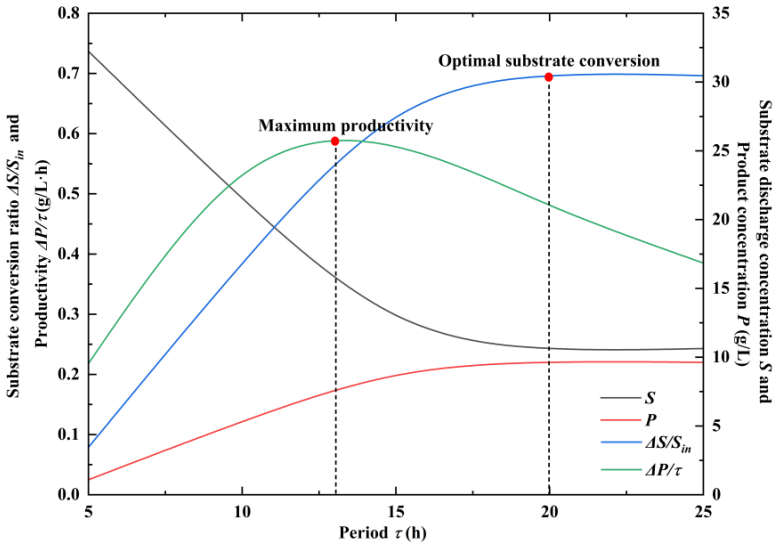

Figure 3. Simulation of periodic on/off switching operation with varying period.

To compare the over-yield potential with the steady-state counterpart, simulations were carried out by varying the discharge-and-reload ratio and the periodicity. The maximum specific dilution rate is set as $D_{\max} = 0.3$ h^{-1}, A fermentation tank with a volume of 100 m^3 is considered. As shown in **Figure 4**, approximately $ave(D) = 0.106$ h^{-1} represents a turning point, and a higher dilution rate enables the on/off switching operation to outperform the corresponding steady-state operation. For a given periodicity, changes in the average dilution rate, $ave(D)$, cause the discharge-and-reload ratio r to vary, as depicted in the bar graph in **Figure 4a**. It can be observed that an increase in r enhances substrate consumption during on/off switching operations. However, an excessive replacement of the fermentation broth may lead to a stationary phase where cell metabolism ceases. Here, we recommend that r be approximately 50% (v/v) because the starting conditions for the next batch

cycle will then be close to the maximum specific growth rates. From **Figure 4b**, it can be verified that minimizing substrate loss and maximizing product yield are two sides of the same coin (Bayen et al., 2020). Consequently, we will focus solely on the substrate conversion problem.

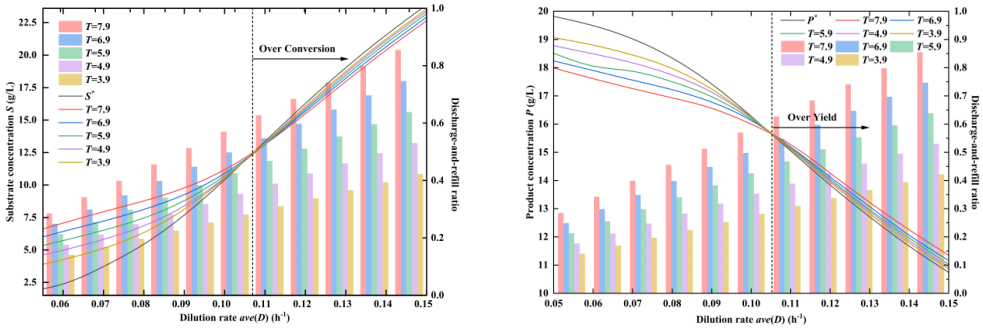

(a) **(b)**

Figure 4. Substrate and product state change with varying discharge-and-reload ratio and periodicity, where over-yield of product or over conversion takes place when $ave(D) = 0.106$ h^{-1}. **(a)** The substrate change under varying discharge-and-reload ratio and periodicity; **(b)** The product change under varying discharge-and-reload ratio and periodicity.

4.3. Discussion on batch-to-batch fermentation through on/off switching operations

Based on the above computations, over-yield occurs when the average dilution rate, $ave(D) > 0.106$ h^{-1}. However, this may also result in a high level of substrate loss. Thus, in practical applications, it is essential to consider substrate depletion as an additional condition. We assume that at the end of each batch period, the substrate concentration returns to the anchor equation $S(t_2^-) = S_{\min}$, where $S_{\min}$ represents the allowable substrate discharge content. Once the substrate content decreases to $S_{\min}$, the on/off switching action is initiated. Evidently, the discharge-and-reload ratio is related to the initial substrate content of the next batch cycle, and we can utilize the above-mentioned analysis methods to design the periodicity.

Without loss of generality, for subsequent analysis, we set $S_{\min} = 0.5$ g/L. The analytical solution of Eq. (24) gives:

$$S(t_2) = S(t_1^+) + \sum_{i=1}^{2} \nu(S)\big|_{S(t_1^+)} V_i(t) + \sum_{i,j=1}^{2} L_\nu \nu(S)\big|_{S(t_1^+)} V_{ij}(t) + \sum_{i,j,i=1}^{2} L_\nu L_\nu \nu(S)\big|_{S(t_1^+)} V_{ijl}(t) \tag{42}$$

where $S(t_2) = S_{\min}$ is the anchor equation. Any admissible initial value $S(t_1^+)$ in Equation (42) determines a fixed time-interval for the fermentation process to convert the substrate from the initial $S(t_1^+)$ to $S_{\min}$. The switch-off operation and the fermentation duration take place within the time interval $[t_1 = 0, t_2]$.

Subsequently, the on/off switching operation is carried out with $D = D_{\max}$ to change the state from $S_{\min}$ to $S(t_1^+)$, which is given by:

$$\begin{aligned} S(\tau + t_1) = S(t_2) &+ \sum_{i=1}^{2} (f + u_i g)\big|_{S(t_2)} V_i(t) \\ &+ \sum_{i,j=1}^{2} L_{f+u_i g}(f + u_i g)\big|_{S(t_2)} V_{ij}(t) \\ &+ \sum_{i,j=1}^{2} L_{f+u_i g} L_{f+u_j g}(f + u_i g)\big|_{S(t_2)} V_{ijl}(t) \end{aligned} \tag{43}$$

where $u_1 = D_{\max} = 0.3\ \text{h}^{-1}$ and $u_2 = D_{\min} = 0\ \text{h}^{-1}$. Then, during the discharge-and-reload process, the fermentation culture is replaced. With the ratio r, we can calculate the new state as $S(\tau) = (1 - r)S_{\min} + rS_{in}$. The start of the next switching cycle, within the time interval $[t_2, \tau]$, for the termination state to change from $S_{\min}$ to $S(t_1^+)$ can be computed using Eq. (43).

For any given initial value $S(t_1^+)$, we can determine the periodicity, and consequently, the productivity and the substrate conversion ratio. As shown in **Figure 5**, for a fixed substrate input concentration $S_{in} = 50$ g/l, the optimal periodicity is $\tau = 6.85$ h. At this point, the overall productivity is approximately 0.97 [g/L h], and the substrate conversion rate reaches 97.1%. In fact, if $S_{\min}$ is set at a low value, a high substrate conversion ratio can be ensured. Note that for this optimal on/off switching strategy, the discharge-and-reload ratio is approximately 50% (w/w), thus validating the SCF strategy. It should be noted that SCF is a viable strategy because the starting condition for each cycle is close to the maximum specific growth rates.

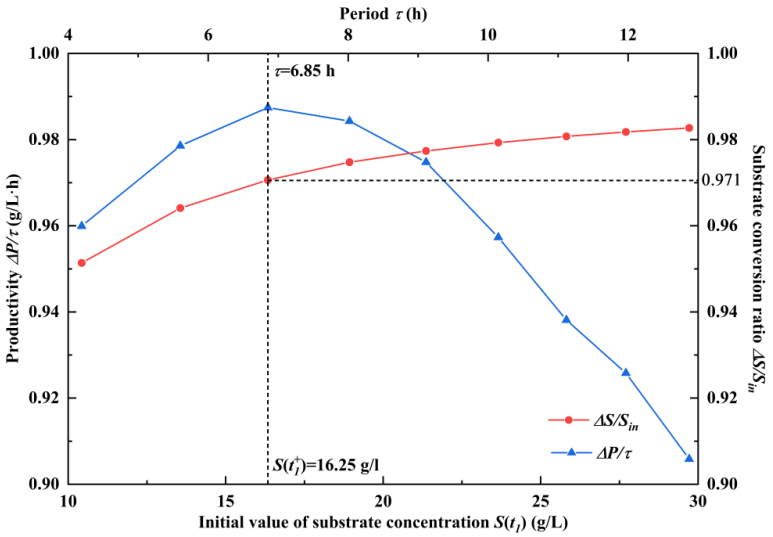

Figure 5. The optimal on/off switching strategy for different initial values of the substrate concentration.

It is important to note that S_{in} can be one of the manipulated variables in the optimal strategy design. By increasing the concentration of the substrate supply, the initial content $S(t_1^+)$ increases. From **Figure 6**, we can observe that both the productivity and the conversion ratio increase significantly due to the high efficiency of the discharge-and-reload actions. For example, when $S_{in} = 100$ g/l, the optimal periodicity is $\tau = 11.9$ h. At this time, the overall productivity reaches 1.432 [g/l h],

the substrate concentration after replacement is 38.48 g/l, and the substrate conversion is approximately 98.6%.

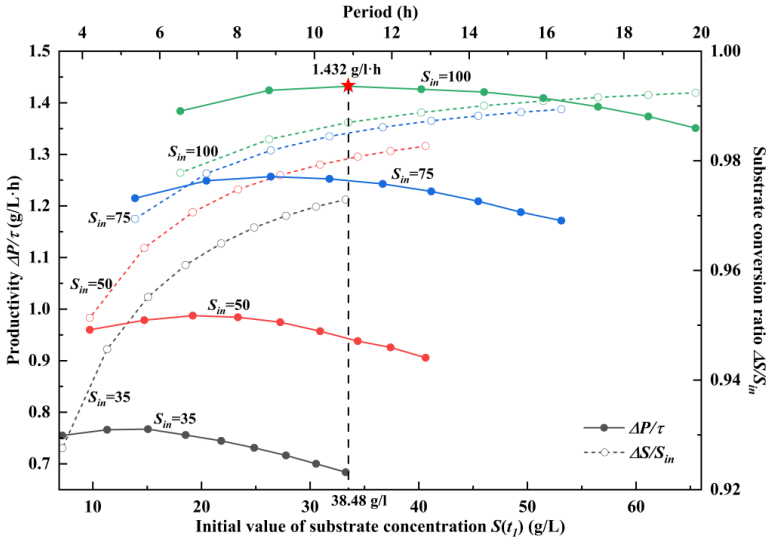

Figure 6. The optimal on/off switching strategy with varying input substrate concentration S_{in}.

Next, to evaluate the superiority of our strategy, the annual production under the optimal on/off switching strategy (with states marked by pentacles in **Figure 6**) is compared with that of the batch-mode. For a reactor with a working volume (V) of $10^5 l$, the downtime between each batch is estimated to be 6h ($t_{d-batch}$) [39]. Given an average of 7920 working hours per year and an estimated batch time of 30 h ($t_{f-batch}$), **Figure 2a** shows that the production per batch is $C_b = 41.08$ g/l/campaign of ethanol. Then, the annual production for N_b campaigns is calculated as:

$$\begin{aligned} N_b &= \frac{t_{annual}}{t_{d-batch} + t_{f-batch}} \\ &= \frac{7920\,h/year}{30\,h/campaign + 6\,h/campaign} \\ &= 220\,campaign/year \end{aligned} \tag{44}$$

Correspondingly, the annual ethanol productivity for batch fermentation (P_b) is:

$$\begin{aligned} P_b &= N_b \times C_b \times V \\ &= 220\,campaign/year \times 41.08\,g/l/campaign \times 10^5\,l \\ &= 903\,ton/year \end{aligned} \tag{45}$$

While for the batch-to-batch production using the autonomous on/off switching strategy, with a maximum productivity of 1.432 g/L·h), the annual ethanol productivity for SCF fermentation P_{SCF} is:

$$\begin{aligned} P_{SCF} &= t \times C_{SCF} \times V \\ &= 7920\,h/year \times 1.432\,g/(l \cdot h) \times 10^5\,l \\ &= 1134\,ton/year \end{aligned} \tag{46}$$

Compared to the annual productivity of batch fermentation (903 tonne/a), the annual productivity of our proposed strategy reaches 1134 tonne/a, representing a 25.58% improvement.

5. Conclusions

This study presents a rigorous framework for optimal cycling strategy of nonlinear input-affine systems, characterized by integral constraints on inputs and periodic boundary conditions. The proposed on-off switching strategy extends existing results to multidimensional systems with arbitrary initial states, offering a systematic approach to design piece wise-constant laws that minimize time-averaged outputs while enforcing oscillatory trajectories. By discretizing the periodic orbit and leveraging the analytical structure of input-affine dynamics, the problem is transformed into a nonlinear optimization formulation where inputs and sub-interval duration are optimized under constraints using Fliess functional expansion, which decomposes system solutions into nested series of Lie brackets, enabling the explicit construction of periodic trajectories through recursively structured compositions of vector fields. The derived anchor equation links design parameters to trajectory geometry, ensuring consistency with the system's dynamics and periodicity requirements.

The framework is validated in successive batch-to-batch ethanol fermentation processes, an archetypal nonlinear system with industrial relevance. Using an experimentally calibrated model, the strategy systematically designs periodic trajectories with precise control over duty cycles and switching instants, demonstrating convergence to stable periodic orbits under external forcing. Performance comparisons reveal a 25.58% improvement in time-averaged productivity (e.g., ethanol yield per cycle) relative to conventional batch-mode operations. This efficiency gain arises from leveraging the system's affine structure through bang-bang control, which optimally exploits the input values to minimize averaged outputs within the constraint of fixed cumulative input effort.

Author contributions: Conceptualization, CZ; methodology, WL and CZ; software, CZ; validation, WL and CZ; formal analysis, WL and CZ; investigation, WL; resources, CZ; data curation, CZ; writing—original draft preparation, WL and CZ; writing—review and editing, CZ; visualization, WL and CZ; supervision, CZ; project administration, CZ; funding acquisition, CZ. Both authors have read and agreed to the published version of the manuscript.

Funding: The authors gratefully acknowledge the following institutions for their support: "Xingdian Talent Support Plan" of Yunnan Province (Grant No.KKRD202205037); Open Foundation of Yunnan Key Laboratory of Intelligent Control and Application (Grant No.2025ICA05); Yunnan Major Scientific and Technological Projects (Grant NO. 202202AG050001).

Data availability statement: All data generated or analyzed during this study are included in this published article.

Acknowledgement: We would like to thank the editors and the reviewers for their

constructive comments and valuable suggestions, which helped to improve the paper.

Conflict of interest: The authors have no relevant financial or non-financial interests to disclose.

References

1. Meadows T, Wolkowicz GS. Competition in the nutrient-driven self-cycling fermentation process. Nonlinear Analysis: Hybrid Systems. 2024; 54: 101519. doi: 10.1016/j.nahs.2024.101519
2. Tian Y, Sun K, Chen L, et al. Studies on the dynamics of a continuous bioprocess with impulsive state feedback control. Chemical Engineering Journal. 2010; 157(2–3): 558–567. doi: 10.1016/j.cej.2010.01.002
3. Zhai C, Palazoglu A, Wang S, et al. Strategies for the analysis of continuous bioethanol fermentation under periodical forcing. Industrial & Engineering Chemistry Research. 2017; 56(14): 3958–3968. doi: 10.1021/acs.iecr.6b03930
4. Silveston PL, Budman H, Jervis E. Forced modulation of biological processes: A review. Chemical Engineering Science. 2008; 63(20): 5089–5105. doi: 10.1016/j.ces.2008.06.017
5. D'Avino G, Crescitelli S, Maffettone PL, et al. On the choice of the optimal periodic operation for a continuous fermentation process. Biotechnology progress. 2010; 26(6): 1580–1589. doi: 10.1002/btpr.461
6. Gilbert EG. Optimal periodic control: A general theory of necessary conditions. SIAM Journal on Control and Optimization. 1977; 15(5): 717–746. doi: 10.1137/0315046
7. Zhai C, Palazoglu A, Sun W. A study of periodic operation in bioprocess systems: Internal and external oscillations. Computers & Chemical Engineering. 2020; 133: 106661. doi: 10.1016/j.compchemeng.2019.106661
8. Bailey JE, Horn FJM. Comparison between two sufficient conditions for improvement of an optimal steady-state process by periodic operation. Journal of Optimization Theory and Applications. 1971; 7: 378–384. doi: 10.1007/BF00934000
9. Bayen T, Rapaport A, Tani FZ. Improvement of performances of the chemostat used for continuous biological water treatment with periodic controls. Automatica. 2020; 121: 109199. doi: 10.1016/j.automatica.2020.109199
10. Bittanti S, Fronza G, Guardabassi G. Periodic control: A frequency domain approach. IEEE Transactions on Automatic Control. 1973; 18(1): 33–38. doi: 10.1109/TAC.1973.1100225
11. Sterman LE, Ydstie BE. Periodic forcing of the CSTR: An Application of the generalized II-criterion. AIChE journal. 1991; 37(7): 986–996. doi: 10.1002/aic.690370704
12. Parulekar SJ. Systematic performance analysis of continuous processes subject to multiple input cycling. Chemical engineering science. 2003; 58(23–24): 5173–5194. doi: 10.1016/j.ces.2003.07.014
13. Kravaris C, Dermitzakis I, Thompson S. Higher-order corrections to the pi criterion using center manifold theory. European journal of control. 2012; 18(1): 5–19. doi: 10.3166/ejc.18.5-19
14. Nikolić D, Seidel-Morgenstern A, Petkovska M. Nonlinear frequency response analysis of forced periodic operation of non-isothermal CSTR with simultaneous modulation of inlet concentration and inlet temperature. Chemical Engineering Science. 2015; 137: 40–58. doi: 10.1016/j.ces.2015.06.018
15. Zhai C, Sun W, Palazoglu A. Analysis of periodically forced bioreactors using nonlinear transfer functions. Journal of Process Control. 2017; 58: 90–105. doi: 10.1016/j.jprocont.2017.08.016
16. Hatzimanikatis V, Lyberatos G, Pavlou S, et al. A method for pulsed periodic optimization of chemical reaction systems. Chemical engineering science. 1993; 48(4): 789–797. doi: 10.1016/0009-2509(93)80144-F
17. Cinar A, Deng J, Meerkov SM, et al. Vibrational control of an exothermic reaction in a CSTR: theory and experiments. AIChE journal. 1987; 33(3): 353–365. doi: 10.1002/aic.690330302
18. Bellman R, Bentsman J, Meerkov SM. Vibrational control of systems with Arrhenius dynamics. Journal of mathematical analysis and applications. 1983; 91(1): 152–191. doi: 10.1016/0022-247X(83)90099-9
19. Benner P, Seidel-Morgenstern A, Zuyev A. Periodic switching strategies for an isoperimetric control problem with application to nonlinear chemical reactions. Applied Mathematical Modelling. 2019; 69: 287–300. doi: 10.1016/j.apm.2018.12.005
20. Guilmeau T, Rapaport A. Singular arcs in optimal periodic controls for scalar dynamics and integral input constraint. Journal of Optimization Theory and Applications. 2022; 195(2): 548–574. doi: 10.1007/s10957-022-02095-y
21. Zhang X, Yuan R. A stochastic chemostat model with mean-reverting Ornstein-Uhlenbeck process and Monod-Haldane response function. Applied Mathematics and Computation. 2021; 394: 125833. doi: 10.1016/j.amc.

2020.125833
22. Dashkovskiy S, Slynko V. Stability conditions for impulsive dynamical systems. Mathematics of Control, Signals, and Systems. 2022; 34(1): 95–128. doi: 10.1007/s00498-021-00305-y
23. Smith R. Impulsive differential equations with applications to self-cycling fermentation [PhD thesis]. McMaster University; 2001. Available online: https://macsphere.mcmaster.ca/bitstream/11375/6197/1/fulltext.pdf
24. Das BK, Sahoo D, Samanta GP. Impact of fear in a delay-induced predator–prey system with intraspecific competition within predator species. Mathematics and Computers in Simulation. 2022; 191: 134–156. doi: 10.1016/j.matcom.2021.08.005
25. Pang G, Sun X, Liang Z, et al. Impulsive state feedback control during the sulphitation reaction in process of manufacture of sugar. International Journal of Biomathematics. 2020; 13(08): 2050076. doi: 10.1142/S179352452050076X
26. Zhang T, Ma W, Meng X. Global dynamics of a delayed chemostat model with harvest by impulsive flocculant input. Advances in Difference Equations. 2017; 1–17. doi: 10.1186/s13662-017-1163-9
27. Yang J, Tan Y, Cheke RA. Complex dynamics of an impulsive chemostat model. International Journal of Bifurcation and Chaos. 2019; 29(08): 1950101. doi: 10.1142/S0218127419501013
28. Tan Y, Agustin RVC, Stein LY, et al. Transcriptomic analysis of synchrony and productivity in self-cycling fermentation of engineered yeast producing shikimic acid. Biotechnology Reports. 2021; 32: e00691. doi: 10.1016/j.btre.2021.e00691
29. Wang J, Chae M, Sauvageau D, et al. Improving ethanol productivity through self-cycling fermentation of yeast: a proof of concept. Biotechnology for biofuels. 2017; 10: 1–11. doi: 10.1186/s13068-017-0879-9
30. Wang J, Chae M, Beyene D, et al. Co-production of ethanol and cellulose nanocrystals through self-cycling fermentation of wood pulp hydrolysate. Bioresource Technology. 2021; 330: 124969. doi: 10.1016/j.biortech.2021.124969
31. Zhai C, Wu S, Chen S, et al. Periodic on-off operations of the self-cycling ethanol fermentation process: Stability analysis and optimal operation strategies. Chemical Engineering and Processing-Process Intensification. 2024; 200: 109805. doi: 10.1016/j.cep.2024.109805
32. Fliess M, Lamnabhi M, Lamnabhi-Lagarrigue F. An algebraic approach to nonlinear functional expansions. IEEE transactions on circuits and systems. 1983; 30(8): 554–570. doi: 10.1109/TCS.1983.1085397
33. Batigün A, Harris KR, Palazoğlu A. Studies on the analysis of nonlinear processes via functional expansions—I. Solution of nonlinear ODEs. Chemical Engineering Science. 1997; 52(18): 3183–3195. doi: 10.1016/S0009-2509(97)00117-6
34. Zuyev A, Grushkovskaya V. Motion planning for control-affine systems satisfying low-order controllability conditions. International Journal of Control. 2017; 90(11): 2517–2537. doi: 10.1080/00207179.2016.1257157
35. Wu S, Chen S, Zhai C. Design and repetitive control of a self-cycling ethanol fermentation bioreactor for ethanol production. Journal of Process Control. 2025; 148: 103403. doi: 10.1016/j.jprocont.2025.103403
36. Astudillo ICP, Alzate CAC. Importance of stability study of continuous systems for ethanol production. Journal of biotechnology. 2011; 151(1): 43–55. doi: 10.1016/j.jbiotec.2010.10.073
37. Wang J, Chae M, Bressler DC, et al. Improved bioethanol productivity through gas flow rate-driven self-cycling fermentation. Biotechnology for biofuels. 2020; 13: 1–14. doi: 10.1186/s13068-020-1658-6
38. Ferrell JE, Tsai TY-C, Yang Q. Modeling the cell cycle: why do certain circuits oscillate? Cell. 2011; 144(6): 874–885. doi: 10.1016/j.cell.2011.03.006
39. Feng S, Srinivasan S, Lin YH. Redox potential-driven repeated batch ethanol fermentation under very-high-gravity conditions. Process Biochemistry. 2012; 47(3): 523–527. doi: 10.1016/j.procbio.2011.12.018